Proceedings of ASME Turbo Expo 2019: Turbomachinery Technical Conference and Exposition
GT2019
June 17-21, 2019, Phoenix, AZ, USA

GT2019-90437

HIGH POWER STEAM TURBINE LIFETIME INCREASE BY MEANS OF FRONT END SEAL ARRANGEMENT AND START-UP HEATING CONDITIONS IMPROVEMENT

Dr. Leonid Moroz
SoftInWay Inc.
1500 District Ave, Burlington, MA 01803, USA
L.Moroz@softinway.com

Dr. Roman Kochurov
SoftInWay Inc.
1500 District Ave, Burlington, MA 01803, USA
R.Kochurov@softinway.com

Dr. Julija Bakhmutska
A. Pidgorny Institute for Mechanical Engineering Problems
2/10 Pozharsky St., Kharkiv, 61046, Ukraine
Julia.Bakhmutska@gmail.com

Dr. Vladimir Goloshchapov
A. Pidgorny Institute for Mechanical Engineering Problems
2/10 Pozharsky St., Kharkiv, 61046, Ukraine
V.N.Goloshapov@gmail.com

ABSTRACT

Use of high power steam turbines in maneuver regimes by power plants became a widely-distributed practice in chase of short-term economic benefits. At the same time, these actions resulted in much higher levels of lifetime consumption for turbines which are not designed for high numbers of start-ups.

The purpose of the present study is to improve operational flexibility for 325 MW steam turbine through design modifications.

For the accurate simulation of rotor thermo-structural state and lifetime, an improved methodology was developed. The approach allows engineers to account for the steam film condensation process and the steam flow physics for regions with the anticipated high-stress levels at front-end seal zone, and the influence of the inter-casing space steam film condensation on the flow parameters in the front-end seals chambers.

Based on the simulation results for the 325 MW supercritical steam turbine HP rotor, the design changes of the front-end seal arrangement and heating conditions modification during the pre-warming phase are proposed. The results show that the proposed changes make it possible to provide a more uniform heating and lower thermo-stress level for the high-pressure cylinder rotor at the front-end seal region during the pre-warming phase, which results in an increased allowable number of turbine start-ups.

The influence of heating conditions on thermo-stresses and low cycle fatigue lifetime for the baseline and modified designs as well as modeling details for transient thermo-structural analysis have been discussed.

INTRODUCTION

The evolution of the energy market in past years has resulted in a change of the principals in power plant operation. The increase of solar and wind power plant numbers has led to significant fluctuation of power generation. To fill the gaps of fluctuation, power generation operators are forced to start and shut down steam turbines frequently to compete in today's market. The energy sectors of many countries experience the lack of peaking power generating units. Use of high power steam turbines in maneuver regimes became a widely-distributed practice, which gives short-term economic benefits. The majority of high power 150-300 MW steam turbines have been designed for continuous operation and steady load. The frequent start-up/shut down events for these machines result in much higher levels of the lifetime consumption of main turbine components.

Operational flexibility of the steam turbines became a strong requirement in the modern energy market. In view of this, turbine manufacturers must improve existing steam turbine capabilities, providing increased maneuver characteristics. The methodologies applied to assess and optimize steam turbine rotor life as well as the design improvement areas are presented in [1].

The number of start-ups of the steam turbine is limited by high-temperature components low cycle fatigue (LCF), which is the result of thermal cycling during transients, while the creep-fatigue is the concern when analyzing turbine life during steady-state operation. During start-up/shut down, steam turbine thick-walled components, besides the centrifugal and pressure loading, experience temperature transients, which cause thermal gradients and stresses. Repetitive start-up/shut down events result in low cycle fatigue (LCF), which depends on the magnitude and frequency of thermo-mechanical stresses.

The steam turbine transient operation is usually very complex with regards to the thermal and stress-strain state prediction. Accurate simulation of the thermal boundary conditions during transient operation and thermo-stresses is essential for the correct assessment of an allowable number of start-up cycles and the development of safe turbine design. Such effects as steam film condensation on components surfaces, which takes place at cold start-up, physics of the steam flow in turbine end seals, 'windage' heating in LP cylinder, accounting for 'wet' vs. 'dry' steam properties, etc. can't be ignored [2]. The integrated approach for the turbine components thermal, thermo-structural and lifetime analyses was developed and validated based on the 30 MW steam turbine in [2], [3].

A lot of studies were carried out to analyze thermal stresses during transient operation and improve start-up performance of steam turbine components. The detailed description of the method for the transient thermal analysis of a steam turbine rotor is presented in [4]. One of the methodological aspects discussed in the study is thermal BC simulation for turbine components during transients. The authors made the conclusion that the approaches, which are based on scaling to each time step of the design point HTC proportionally to pressure and temperature ratios, bring errors at some transients. In [3], the brief review of studies conducted before 2017 as well as the algorithm for steam film condensation on component surfaces is given.

Recent studies, performed after 2017 are given below. In [5], recommendations to improve the quick startup performance and decrease the LCF life consumption for 50 MW solar steam turbine are discussed based on start-up simulation, employing simplified FE models. Thermo-structural transient simulation with the focus on casing deformations was performed in [6] for HP casing during shutdown of CPR1000 nuclear steam turbine and a good correlation between calculated and monitoring data was achieved. The applicability of quasi-stationary theory for the valve body thermo-structural analysis during the warm-up process have been discussed in [7].

The current work presents the further improvement of the integrated approach for steam turbine components transient thermo-structural and lifetime analyses, which enables improved accuracy of the simulation results. The approach has been applied to increase the allowable start-up number for 325 MW steam turbine and the following tasks are considered:

1) The methodology for steam turbine thermo-structural analysis at transient operation improvement to increase the accuracy of the results by
(a) Steam film condensation on components surfaces simulation (film condensation conditions calculation methodology; the algorithm for determination of start and end time of the film condensation process);
(b) Detailed simulation of the steam flow physics in the front-end seal zone;
(c) Flow parameters determination in seal chambers taking into the account inter-casing space film condensation;
2) Steam turbine heating conditions and design improvements development to reduce rotor thermal stresses;
3) Simulation of the thermo-stress state and lifetime for baseline and improved designs applying the developed methodology. Proposed changes influence on the steam turbine low cycle fatigue life estimation.

Based on the simulation results for 325 MW steam turbine HP rotor, design changes for the front-end seal carrier and heating conditions modification during the pre-warming phase are proposed. Heating conditions effect on thermo-stresses and LCF lifetime for the baseline and modified designs were estimated. The results show that proposed changes provide more uniform heating and a lower thermo-stress level for the HP rotor at front-end seal region during the pre-warming phase and increased allowable number of turbine start-ups. The influence of the steam film condensation and detailed steam jet flow simulation at the front-end seal zone have been discussed.

NOMENCLATURE

BC – boundary conditions;
CFD – computational fluid dynamics;
CS – cold start-up;
FE – finite element;
FEA – finite element analysis;
FP – flow path;
HP – high-pressure;
HTC – heat transfer coefficient;
HS – hot start-up;
IP – intermediate pressure;
LCF – low cycle fatigue;
LP – low pressure;
WS – warm start-up;

Symbols

D_h – hydraulic diameter;
G – steam mass flow rate;
V – specific volume;
α – HTC;
λ – thermal conductivity;
μ – dynamic viscosity;
ρ – steam density;
υ – kinematic viscosity;
ω – rotational speed;
Re – Reynold's number;
Pr – Prandtl number.

1. BACKGROUND

The unit under investigation is K-325-23,5 – new supercritical parameters steam turbine (fig. 1a). The unit was developed by JSC "Turboatom" to replace the previous generation of 300 MW turbines, which are used in many countries and produced in quantities of more than 120. The turbine operating parameters for the design point are presented below:

1. Rotor nominal speed 3000 rpm.

2. Steam inlet temperature 540 °C.
3. Steam inlet pressure 23.54 MPa.
4. Condenser pressure 3.65 kPa.

The purpose of the present study is to increase the start-up number for the 325 MW steam turbine through improvement of the design.

The field experience shows that for the significant number of similar units with power 150-300 MW, which was in operation more than 50 k hours, circumferential cracks were observed in the high-temperature rotors at the front-end seals zones and seals behind the control stage [8]. In all cases, cracks were the result of high stresses during turbine start-up in the regions of stress concentrators, such as small fillets, thermo-compensation slots, grooves, etc. The most critical region with regards to LCF cracking is HP rotor front-end seal zone (see Fig. 1b).

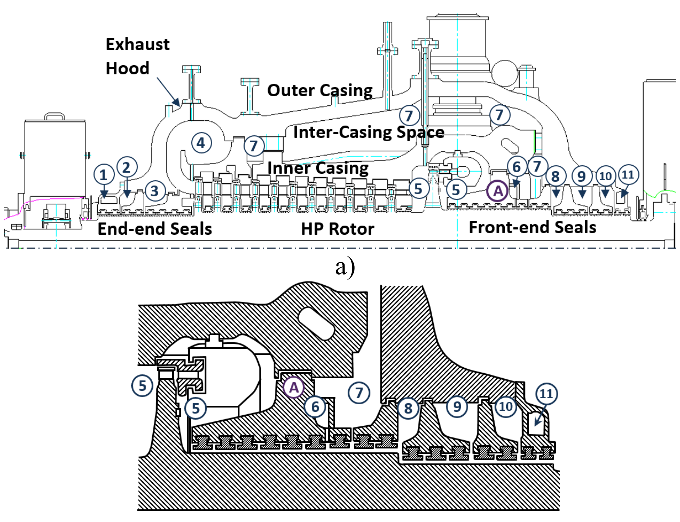

a)

b)

Figure 1: 325 MW Steam Turbine: (a) HP Cylinder Cross Section, (b) Front End Seals Arrangement (Baseline Design)

For the considered steam turbine, the component, which limits LCF lifetime is a HP rotor. This component will be investigated in the current work. The HP rotor (see fig. 1a) is a disk type design, full bore, 4.882 m length, rotor material grade 20H3MVFA. There is a total of 12 stages in the HP cylinder.

Steam turbine start-up/shut down diagrams, which are recommended by OEM were used to simulate transient operation. Turbine pre-warming phase, cold, warm, hot start-ups and shut down were considered in the study. The examples of start-up curves for the turbine pre-warming and cold start-up are presented in Fig.2.

The main focus of the study is the steam turbine start-up from a cold state (initial temperature for the components is less than 150 °C), which is the most interesting operation regime with regards to thermo-structural state and lifetime. Several physical processes take place only during cold start-ups, such as steam film condensation on turbine components surfaces, the significant influence of turbine pre-warming on the level of thermal stresses during start-up, etc.

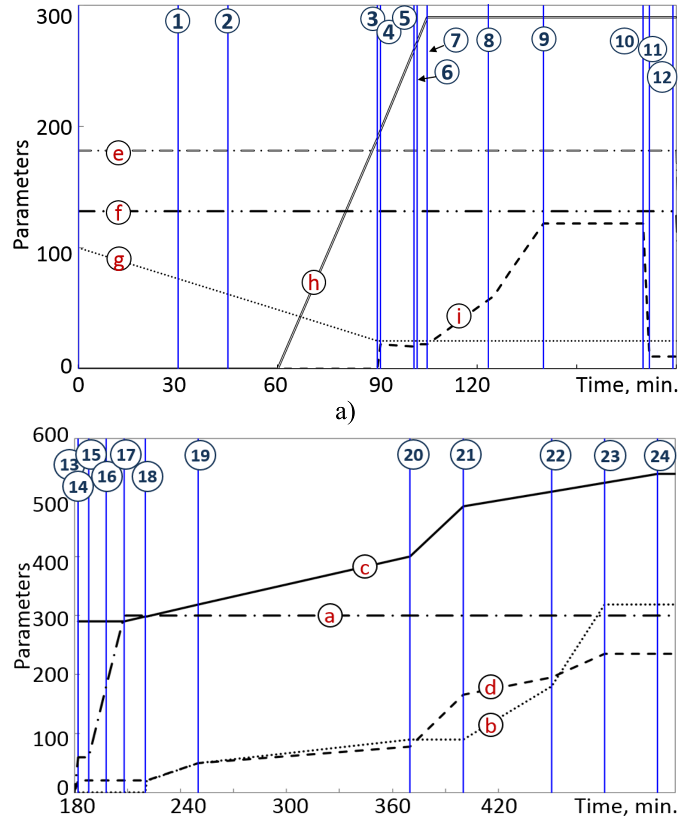

a)

b)

Figure 2: Steam Turbine Pre-Warming (a) and Cold Start-up (b) Diagrams with Simulation Time Steps

(a – rotor speed, rpm; b – power, MW; c, d – FP temperature°C, and pressure, $\cdot 10^{-2}$ kPa; e, f – end seals steam temperature, °C and pressure, $\cdot 10^{-2}$ kPa; g – condenser pressure, $\cdot 10^{-2}$ kPa; h, i – exhaust hood steam temperature, °C and pressure, $\cdot 10^{-3}$ kPa)

Cold start-up with the pre-warming process for the considered steam turbine can be divided into 3 phases. At the first phase (‘reaching the vacuum’, from 0 to 90 min according to Fig. 2a) the steam with the temperature of 180 °C and pressure of 130 kPa comes to the end seals in chambers #2 and #10 (see Fig. 1). The seal's ejectors are activated and the pressure in chambers #1 and #11 is established equal 97 kPa.

At the second phase, from 90 to 180 min, the steam with the temperature of 190 °C flows from the boiler through the cold re-heater steam pipes to exhaust hood. During 15 min steam temperature rises up to 290 °C. From the exhaust hood, the steam follows to the flow path and at 9th stage steam divides into two portions. One portion flows to the inter-casing space through inner casing ring slot and then to the front-end seal chamber #7, while the other portion follows through the turbine stages to the front-end seals. Because of the described specific, the pressure from both sides of the carrier ‘A’ (see Fig. 1b) is almost the same, which results in negligible steam flow between the 5th and 7th front end seal chambers as well as a lack of rotor heating in this region during the whole pre-warming phase. This then leads to overstress of the HP rotor zone under carrier ‘A’ due to excessive thermal gradients present in further steps of cold start-up.

At the third phase of cold start-up, the primary steam goes into the flow path, the rotor starts to spin and rotation speed increases. Next steps are ramping-up to the idle mode, synchronization and reaching the nominal power (see Fig. 2b).

2. IMPROVED METHODOLOGY FOR A STEAM TURBINE THERMAL AND THERMO-STRUCTURAL ANALYSIS

A steam turbine component thermo-structural analysis typically consists of the following steps:

1) Components detailed geometry preparation, thermal zones assignment, and start-up diagram analysis to determine time steps for thermal analysis;
2) Simulation of the steam parameters in turbine flow path and rotor gland seal scheme leakages balance at each time step during a start-up cycle;
3) Thermal BC (HTC and temperatures) simulation for preliminary assigned thermal zones;
4) Transient thermal analysis for casing and rotor components based on thermal BCs;
5) Thermo-structural analysis for a start-up cycle;
6) Components lifetime evaluation.

According to the proposed approach, at the first step of the analysis, the rotor surface was split into thermal zones to simulate heat convection conditions. Zones are determined to have identical or very close boundary conditions within each entire zone. The thermal boundary conditions were simulated for the operation without film condensation as well as for the case of steam film condensation process. Thermal zones are shown on the HP rotor fragment in Fig. 3.

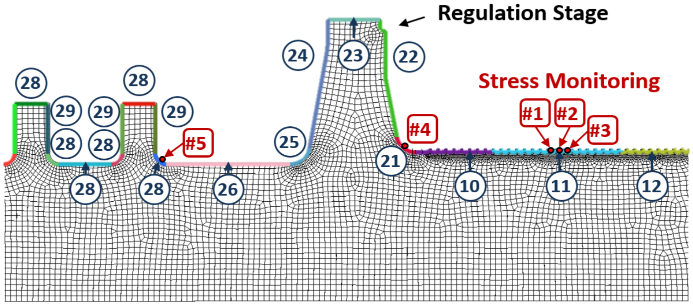

Figure 3: HP Rotor Fragment with Heat Convection Zones

Based on the start-up regimes analysis, the characteristic time moments, which correspond to the turbine start-up parameters (steam temperature, pressure, rotor speed, etc.) change, are selected. The time moments for the pre-warming and cold start-up operation are presented in Fig. 2 by vertical lines.

For each determined time step, steam parameters and flow characteristics in the flow path, rotor gland seals/chambers, and inter-casing space were calculated in AxSTREAM NET™ tool, which is based on the 1D approach and enables analysis of

- flow characteristics at off-design modes;
- main stream and leakages balance solution for the turbine flow path integrated with gland seal system and inter-casing space;
- the hydraulic resistance of the drainage system elements, bypass steam pipes;
- account for 'dry' and 'saturated' steam properties and temperature rise because of 'Windage'.

The integrated scheme for the baseline variant of the K-325-23,5 steam turbine, which was considered in the study is presented in Fig. 4 and includes a flow path, gland seal system, inter-casing space, and exhaust hood.

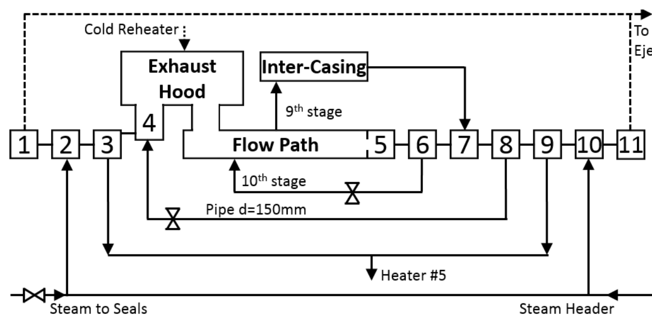

Figure 4: HP Rotor Gland Seals System (Baseline Design)

Fragments of the entire scheme for the flow characteristics simulation are presented in Fig. 5. The solution (flow characteristics) for each element was generated for nominal and off-design modes.

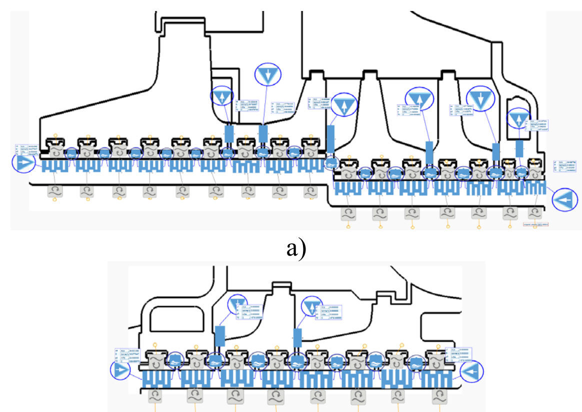

a)

b)

Figure 5: Flow Characteristics Simulation in HP: a) Front End Seals; b) Rear End Seals

For K-325-23,5 steam turbine at the pre-warming phase, the steam is supplied through the HP cylinder exhaust hood to the flow path and then through the slot, after the 9th stage, the steam flows into the inter-casing space. The steam film condensation takes place on the inner and outer casings. When steam film condensation in the inter-casing space is finished, the steam flows to the end seal chamber #7 (see fig. 1). To predict the flow characteristics in end seals chambers during the period of heating through the exhaust hood the heating conditions in inter-casing space were calculated taking into the account the amount of condensed steam on the inner and outer casings before the steam reaches the seals' 7th chamber.

At the third step of the study, thermal BCs were simulated for all assigned rotor surfaces (including flow path, seals, bearings and air convection zones – see Fig. 1a) at each determined time step during transients (from Fig. 2). The BCs of the third kind (HTCs and steam temperatures) for the cases of single-phase flow and steam film condensation have been calculated according to the approach presented below.

HTC simulation for the turbine component surfaces is based on the Dittus-Boelter equation for turbulent pipe flow [9]:

$$Nu = K \cdot Re^m \cdot Pr^n; \quad \alpha = \frac{Nu \cdot \lambda}{D_h}, \tag{1}$$

where K, m, n, – coefficients, determined by convective heat exchange conditions; $Pr = \frac{\upsilon}{\lambda}$; $Re = V_{tot} \cdot D_h/(\upsilon \cdot V)$; $V_{tot} = \sqrt{V_{ax}^2 + V_{rel}^2}$; $V_{rel} = K_1 \cdot \omega \cdot r$; $V_{ax} = \frac{G}{\pi\rho(r_{ext}^2 - r_{in}^2)}$; K_1 – coefficient, influenced by the velocity profile in the gap between rotating and non-rotating surfaces; r – cylindrical surface radius; r_{ext}, r_{in} – external and internal surface radius.

HTCs in the flow path were determined for thermal zones schematically presented in Fig. 6 taking into the account airfoil surface and root influence.

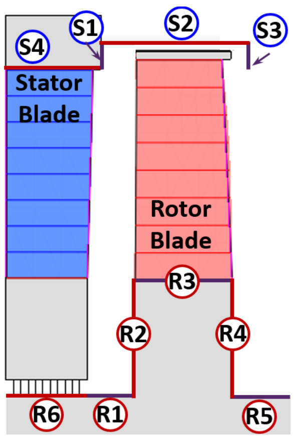

Figure 6: Flow Path Stage Heat Convection Zones Schematization

The more detailed simulation has been done for the front-end seal zone: methodological improvements were made to account physics of the jet flow and turbulent pulsation of the working fluid velocity in sealing groves on the rotor. The approach is based on the experimental studies for heat transfer conditions for the case of inleakage of the semi-restricted stream on the wall, which was done in A. N. Podgorny Institute for Mechanical Engineering Problems NAS of Ukraine [11].

According to the developed approach, in the considered seal groove (Fig. 7): the turbulent semi-restricted stream flow is observed along surface 'A' (see Fig. 7), while to the surface 'B' the stream inleak perpendicularly. At the corner zone, a stagnation of flow is observed.

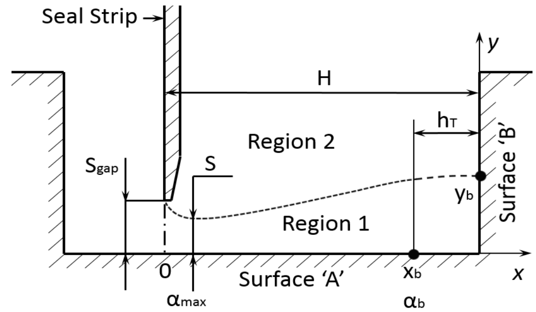

Figure 7: Seal Groove Boundary Points Position

Based on the experimental measurements, the boundary point x_b, which delimits the stagnation zone, was determined and can be calculated as

$$\bar{x}_b = 0{,}72 \cdot \bar{H}, \; \bar{H} = \frac{H}{S}, S = 0{,}85 \cdot S_{gap}, \tag{2}$$

where the geometrical parameters are presented in Fig. 7.

HTCs on the surface 'A' for the zone $0 \le x \le x_b$ were calculated using the formula below

$$Nu_x = 0{,}03 \cdot Re^{0{,}8} \cdot Pr^{0{,}43} \cdot \left(\frac{Pr_f}{Pr_w}\right)^{0{,}25}, \tag{3}$$

where Pr_f, Pr_w – Prandtl numbers calculated for the flow and wall temperatures.

At the stream stagnation zone $x_b \le x \le$ H, HTCs are decreasing according to the relation below

$$\alpha = \alpha_{xb} \cdot (1 - \bar{\bar{x}}^2), \; \bar{\bar{x}} = \frac{x - x_b}{H - x_b}, \tag{4}$$

where α_{xb} – HTC at the boundary point x_b.

On the surface 'B' based on the experimental evaluations, the new correlations for HTC simulation were developed. The new correlations enable increased accuracy of the HTC calculation for the steam turbine end seals zones and are presented below

$$Nu_b = 0{,}37 \cdot (\bar{H})^{-0{,}5} \cdot Re^{0{,}65} \cdot Pr^{0{,}43}; \tag{5}$$

$$\alpha_{yb} = \frac{Nu_b \cdot \lambda}{S_{gap}}; \; Re_{gap} = \frac{U_0 \cdot S_{gap}}{\upsilon}; \; U_0 = \frac{G \cdot V}{\pi \cdot d_t \cdot S}, \tag{6}$$

where d_t – seal socket diameter (under the tooth); α_{yb} – HTC at the boundary point y_b; $y_b = S + H \cdot tg23°$ (based on the experimental data).

HTC at the region of pulsation component influence 'Region 1' (see Fig. 7), when $0 < y \le y_b$ can be calculated using the following formulas

$$\alpha = (1{,}32 - 0{,}112 \cdot \bar{\bar{y}} - 0{,}208 \cdot \bar{\bar{y}}^2) \cdot \alpha_{yb}, \tag{7}$$

$$\bar{\bar{y}} = \frac{y}{y_b}, \bar{y}_b = \frac{y}{S}. \tag{8}$$

HTC at the region on a stable flow of semi-restricted stream along the surface 'B' in the 'Region 2' (from Fig. 7) when $y_i > y_b$ can be determined as

$$Nu_i = Nu_b \cdot \left(\frac{\bar{y}_b}{\bar{y}_i}\right)^{0{,}245}; \; \bar{y}_i = \frac{y_i}{S}, \tag{9}$$

where $\bar{y}_i$ – current relative coordinate in the 'Region 2'.

For the case of the steam film condensation on the component surfaces, the HTCs were calculated using the following relations

$$\bar{\alpha}_{cond} = \frac{3}{2} \cdot \sqrt[3]{\frac{\lambda_f^2 \cdot L_h \cdot c_f^c \cdot \rho_s \cdot U_b^2}{6 \cdot \upsilon_f \cdot l_i \cdot (T_s - \mathrm{T}_w)}}; \tag{10}$$

$$U_b = \left(\frac{1{,}5 \cdot S_{bl} \cdot l_i^{0{,}5}}{\upsilon_f^{0{,}5} \cdot \rho_f}\right)^{2/3}, \tag{11}$$

where λ_f – fluid thermal conductivity; L_h – condensation heat at a given pressure; c_f^c – friction coefficient on the interfacial vapor-liquid surface; ρ_s – steam density; υ_f – kinematic the viscosity of the condensed steam; l_i – surface length; T_s, T_w – saturation and wall temperatures; U_b – steam and condensation film velocity at the boundary between phase split; S_{bl} – condensation film thickness; ρ_f – condensed steam density.

Heat transfer conditions in bearings are usually presented as criteria correlations obtained by the method of the similarity theory [11]:

$$Nu = F\left(Re_0, Pr_0, K_v, K_p, E_c, \frac{Pr_w}{Pr_0}, \frac{L}{R}, \psi, \frac{\delta_v}{\delta_h}\right); \quad \alpha = \frac{Nu \cdot \lambda}{d}, \tag{12}$$

where $Pr = \frac{\upsilon}{a}$; $Re = \frac{2\omega R_s^2}{\nu_0}$; $K_v = \frac{W}{u}$; $K_p = \frac{P}{S_b \rho u^2}$; $\psi = \frac{\delta}{R_s}$; $u = \omega R_s$; W – oil average flow rate velocity; $W = \frac{G_{oil}}{2\rho\pi d_s(\delta_v + \delta_h)}$; L – bearing length; δ – radial bearing clearance; $\delta = R_s - R_b$; R_s – shaft journal radius; R_b – bearing radius; δ_v, δ_h – average bearing clearances in vertical and horizontal directions; d_s – shaft journal diameter; G_{oil} – oil mass flow rate; P – bearing load; a – thermal diffusivity; indexes '0' and 'w' correspond to parameters determined at T_0 – oil temperature at bearing inlet, or at T_w – shaft surface temperature.

During the steam turbine start-up, depending on the relation between component metal temperature and the steam saturation temperature, the film steam condensation process may take place. The start of the steam turbine film condensation results in a rapid change of heat exchange BCs. The approach, which is based on the interactive analysis of the component surface local temperature and surrounding steam saturation temperature during the heating process, was used in the study to determine whether the film condensation process takes place and which BC shall be used at the particular time step. A detailed description of the thermal analysis algorithm is presented below [2]:

1. The initial thermal state for a turbine component is defined based on the solution for natural cooling from steady state task taking into account the turbine outage time and is used to start the calculation process.

2. The metal temperature of the component's local surface is monitored and compared against the saturation temperature of the steam surrounding this zone (Fig. 3) at each time during start-up.

3. If the metal temperature in the local region is lower than that of steam saturation temperature then film condensation takes place and the corresponding BCs are applied: steam saturation temperature as heating temperature and HTCs calculated for the case of film condensation by equations (10), (11).

4. In another case, when rotor surface temperature is higher than steam saturation temperature, HTCs were calculated with the assumption of single-phase flow and the superheated steam temperature is used for the BCs: equations (1) – (9).

Finite element (FE) method is used to simulate transient thermal and thermo-structural state. 2D axisymmetric FE model based on 8-node quadrilateral plane elements (with axisymmetric option) has been developed for HP rotor transient analyses. Mesh refinements were done in the regions of potential stress concentration, such as fillets, groves at sealing zones, etc., (see Fig. 3) and mesh sensitivity study was performed. Structural BC, centrifugal and pressure loads were considered in the analysis. To estimate the general level of stresses, critical time periods and sufficient time increment for nonlinear stress-strain state simulation, the elastic structural analysis was performed prior to elasto-plastic.

The final step of the study is the LCF and lifetime simulation for the components. LCF analysis is based on the calculated elasto-plastic deformations and experimental stress-strain and strain-life data at room and elevated temperatures for the rotor material [10]. The rotor material assumed to be cyclically hardened and the multi-linear kinematic hardening plasticity model has been applied for the elasto-plastic simulations. The analysis model includes the Bauschinger effect and geometrical nonlinearity. To determine the allowable number of turbine start-ups for the regions with high-stress concentration, the effective strain range $\Delta\varepsilon_{ij}^{el/pl}$ was determined according to the methodology presented in [2]:

$$\Delta\varepsilon_{ij}^{el/pl} = \varepsilon_{ij\,MAX}^{el/pl} - \varepsilon_{ij\,MIN}^{el/pl} \tag{13}$$

where $\varepsilon_{ij\,MAX}^{el/pl}, \varepsilon_{ij\,MIN}^{el/pl}$ – the maximal and minimal elastic/plastic deformations, which were determined from the stabilized stress-strain hysteresis loops for each region of interest.

3. THERMAL AND THERMO-STRUCTURAL ANALYSES RESULTS FOR THE OEM DESIGN

To simulate K-325-23,5 steam turbine HP rotor transient thermal state, thermal BCs were calculated according to the methodology described in paragraph 2. Calculated HTCs distribution on the surface of an end seal segment at nominal operation is presented in Fig. 8. It can be observed that the stream character in gland seal socket as illustrated in ref. [11] resulted in HTCs change in the range from 900 to 5200 W/m²K (calculated applying the developed approach) depending on the flow parameters for the corresponding local regions. The similar detailed BC's simulation was performed for the whole thermal zone '11' from Fig. 3, where the probability of LCF cracking exists.

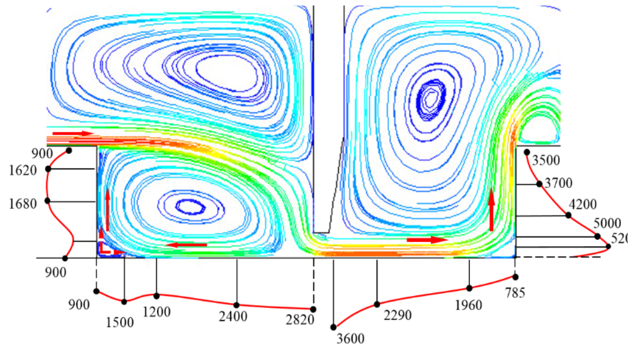

Figure 8: HTC distribution on the Surface of End Seal Segment at Nominal Operation (in W/m^{2}K)

Calculated HP rotor temperature distribution during pre-warming, CS, and steady-state operation for the HP rotor is presented in Fig. 9 and corresponding thermal stresses calculated applying elastic formulation are presented in Fig. 10.

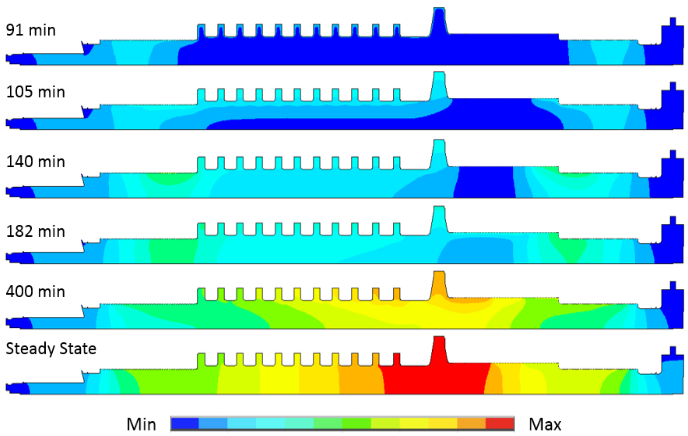

Figure 9: HP Rotor Thermal State during Turbine Pre-Warming and CS

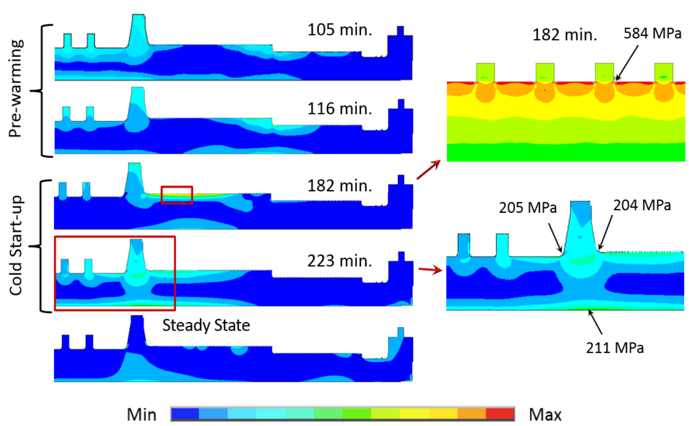

Figure 10: HP Rotor Thermo-Structural State during Turbine Pre-Warming and CS

The thermal analysis results show that at the front-end seals region, high-temperature gradients take place at the time 105, 140 and 182 min. from the beginning of the turbine start-up. Another observation is that the HP rotor portion between chambers 5 and 7 (see Fig. 1) remains cold (the temperature is less than 60 °C) up to the time 180 min. That's why, at 182 min., when the rotor starts to spin, high thermal gradients take place in this region.

To study HP rotor temperatures and thermo-stresses during steam turbine start-up, the control points with stress concentration were selected (see Fig. 11). The temperatures and stresses calculated at these points are presented in Fig. 12.

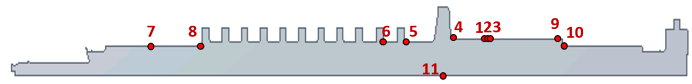

Figure 11: HP Rotor Control Points

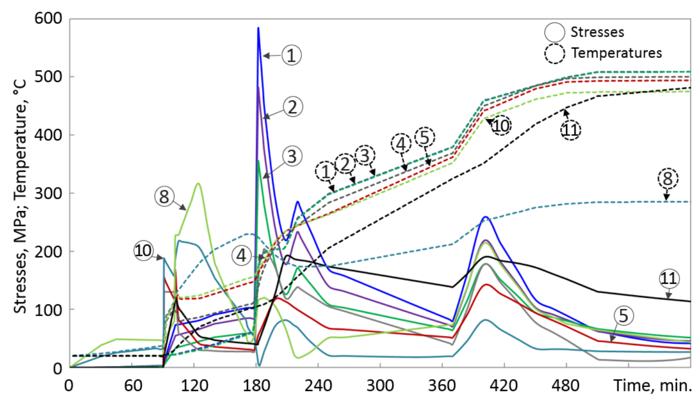

Figure 12: Temperatures and Von Mises Stresses at Control Points during Pre-Warming and CS (Elastic Analysis)

The rapid growth of rotor temperatures during the CS in the region under carrier 'A' (see Fig. 1) is observed from 180 min. when the rotor starts to spin and steam with a temperature of 90 °C flows to the end seals. In less than 10 min., the temperature of the rotor in this area increases from 60 to, almost, 200 °C. During the time the superheated steam flows on the cold rotor portion, the steam film condensation on the rotor surface takes place, which results in a significant intensification of heat exchange and the sudden increase of the metal temperature and thermo-stresses.

Figure 12 shows that rotor maximal stresses appear at point '1' at 182 min. and exceed the yield strength limit for the rotor material at operating temperature. These results confirm that the possibility of LCF cracking exists in the front-end seal region.

Warm and Hot start-up analyses results show that maximal stresses are observed in the rotor bore and much lower than the rotor material yield strength.

The influence of the physical phenomena such as steam film condensation and jet flow physics at front end seals on the stress-strain state is demonstrated in Fig. 13. For the considered design, the difference in maximal von Mises stresses simulated taking into account the steam film condensation and jet flow physics or disregarding the steam film condensation and jet flow physics is ~18% and ~12% respectively (see Fig. 13). Both physical effects result in increased stresses.

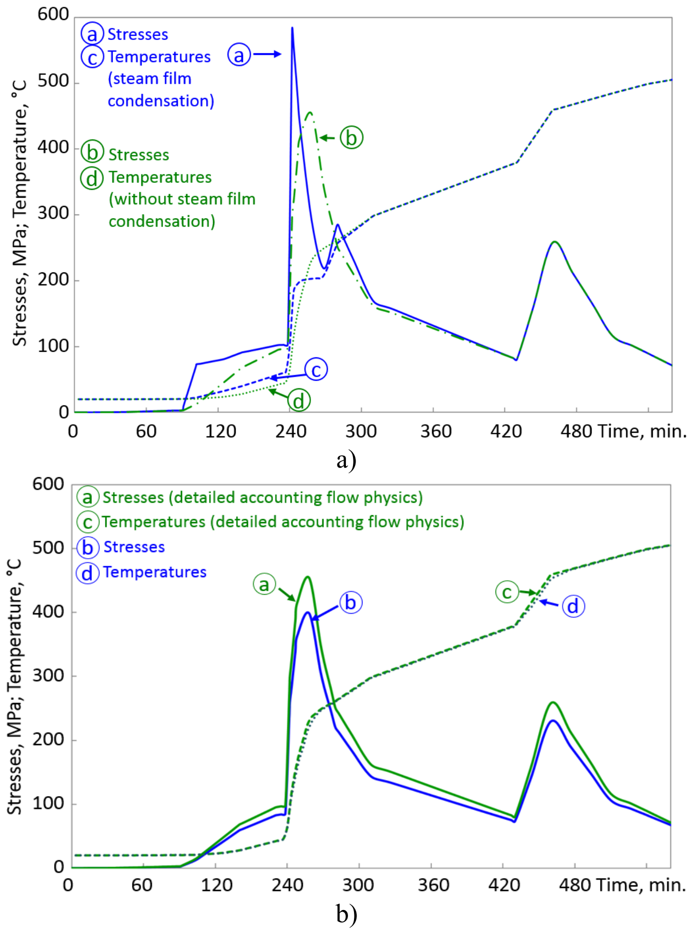

Figure 13: Temperatures and Von Mises Stresses at Control Point '1' Simulated Taking into the Account: (a) Steam Film Condensation, (b) Jet Flow Physics in Rotor End Seals

4. DESIGN MODIFICATION. THERMAL AND THERMO-STRUCTURAL ANALYSES FOR THE IMPROVED DESIGN

The design changes in the front-end seal arrangement and modified start-up heating process have been proposed to provide a more uniform HP rotor heating during the pre-warming and cold start-up phase and overcome potential problems with thermo-stresses and LCF lifetime. The modified design contains additional seal chambers 12 – 14, which are made by insertions in the front seal carrier 'A' (see Fig. 14). These seal chambers are connected to the steam sources of high and low pressure.

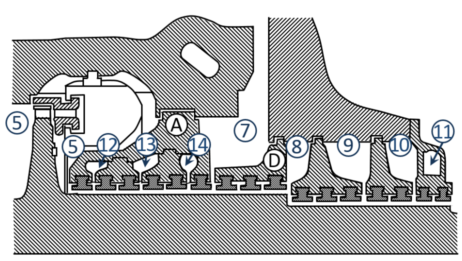

Figure 14: Front End Seals Arrangement (Modified Design)

According to the gland seals operating scheme presented in Fig. 15, during the first 90 min of the pre-warming, steam from steam header also comes to the chambers 8, 12 and 14. Steam parameters for this case are equal to the parameters in chambers 2 and 10 (temperature T = 180 °C, pressure P = 130 kPa). During 90 – 180 min. of the pre-warming phase, the steam goes from cold reheater through the exhaust hood to the 13th chamber similar to the flow path and inter-casing space parameters. Chambers 3, 9, 12 and 14 are connected to the condenser. At the same time, the original start-up process, as well as the seals' teeth numbers, are maintained.

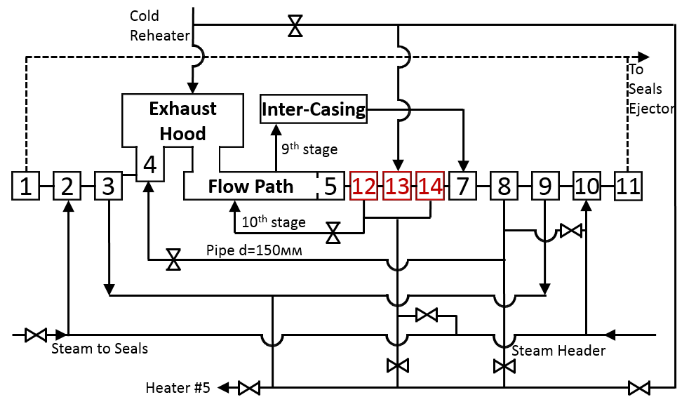

Figure 15: HP Rotor Gland Seals System (Modified Design)

Thus, in the modified design, the rotor portion under seals carrier 'A' heated more uniformly along the whole length of front end seals, due to the better steam circulation between seals chambers '5' and '7', is confirmed by performed simulations of steam flow in end seals sections.

To analyze the effectiveness of the proposed changes in the front-end seal carrier with regards to the HP rotor thermal and structural state, simulations have been performed for the modified design, applying the methodology presented in paragraph 2.

HP rotor thermal state during pre-warming and cold start-up for the modified design are presented in Fig. 16.

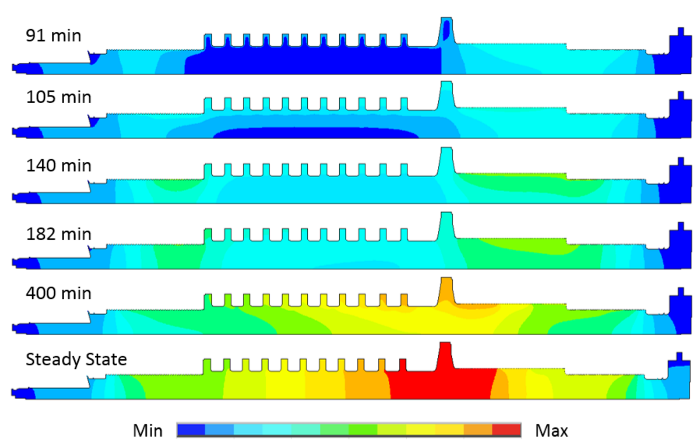

Figure 16: HP Rotor Thermal State during Turbine Pre-Warming and CS (Modified Design)

Thermal analysis results in a modified design show that at the pre-warming phase, rotor portion under carrier 'A' heated more uniformly and intensively in comparison with the baseline design (Fig. 9), where the considered region is cold up to 180 min. from the beginning of the pre-warming process. Because of this, when the rotor starts to spin in the case of the modified design, steam with the temperature of 290 °C flows onto the well pre-heated rotor, which does not result in high thermal gradients and thermo-stresses.

At this step of the study, thermo-structural analysis for the HP rotor is performed in elasto-plastic formulation to estimate total deformations in critical rotor regions and LCF life with high accuracy and compare the results between baseline and modified designs.

The HP rotor elasto-plastic stresses at the front-end seals region during the turbine CS are presented in Fig. 17 for baseline and in Fig. 18 for modified designs.

Equivalent von Mises stresses versus time during turbine pre-warming phase and cold start-up for the monitoring point #1 from Fig. 11 and corresponding metal temperatures at this point are presented for baseline and modified designs in the Fig. 19.

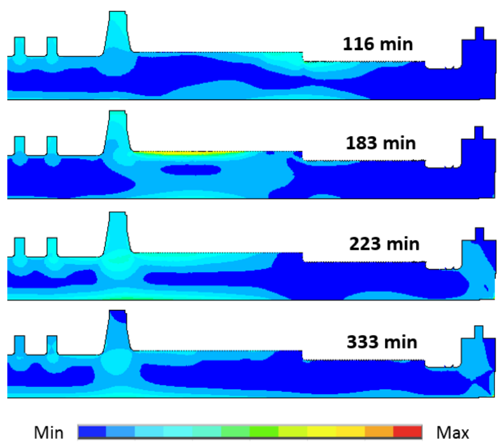

Figure 17: Rotor Von Mises Stresses during CS for Baseline Design

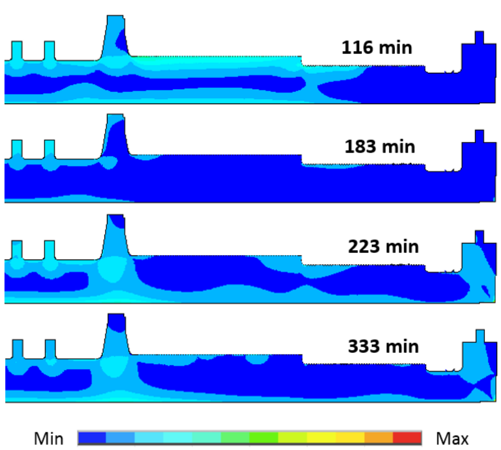

Figure 18: Rotor Von Mises Stresses during CS for Modified Design

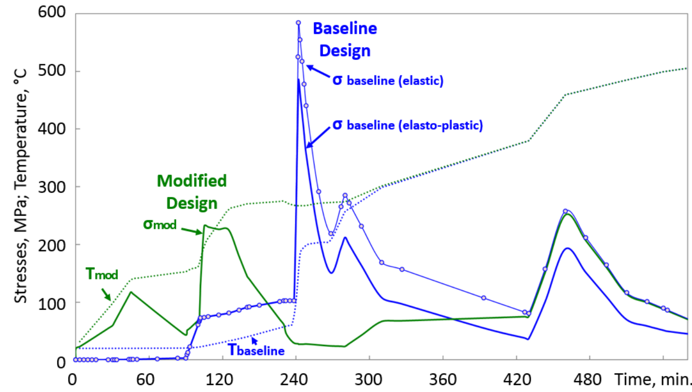

Figure 19: Von Mises Stresses for Baseline and Modified Designs during CS

Maximal thermal stresses for the modified design at the front-seals location (control point '1') correspond to the time of 116 and 400 min. from the beginning of the pre-warming process and are much lower in comparison with the stresses calculated for the original design (the difference is ~53%).

It should be noted that the maximum thermal stresses and deformations of the rotor material are observed during turbine start-up from a cold state as well as the maximal damage due to LCF. The proposed design and heating conditions changes have a maximal influence on HP rotor thermal state also during pre-warming and CS. Because of this, the influence of the proposed changes on the rotor lifetime is analyzed for the following cyclic loading: start-up from the cold state – nominal operation – shut down and natural cooling.

To estimate the influence of the thermal state of proposed design on differential rotor-casing expansions and critical clearance reduction, the difference in absolute HP rotor expansions was analyzed (see Fig. 20). Maximal difference in absolute HP rotor expansions is ~1.5 mm at 150-180 min. from the beginning of the pre-warming phase. After 180 min. (rotor starts to spin) the absolute HP rotor expansions gradually became closer to the baseline design absolute expansions: the difference is 0.5 mm at 221 min. and 0.1 mm at 360 min.

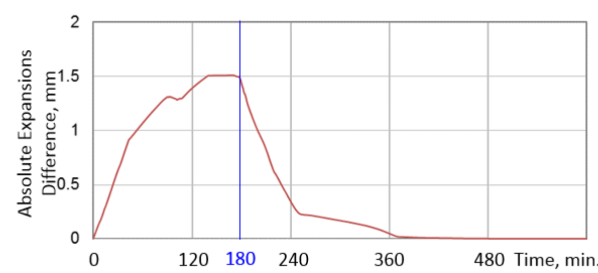

Figure 20: The Difference between Absolute HP Rotor Expansions for the Baseline and Modified Designs

To estimate rotor LCF life, an equivalent effective strain range was calculated based on FE thermo-structural results for the rotor region's possibility of the LCF crack initiation. The number of cold start-up cycles N to LCF crack initiation was calculated using formulas (6) and presented in Table 1 for the monitoring points from Fig. 11 for baseline and modified designs.

$$\mathrm{N} = min\{\mathrm{N}_{aN}, \mathrm{N}_{a\varepsilon}\},\ \mathrm{N}_{aN} = \frac{N(\varepsilon_a)}{K_N},\ \mathrm{N}_{a\varepsilon} = N(\varepsilon_a K_\varepsilon)\ , \quad (6)$$

where ε_a – strain amplitude, $K_N = 5$, $K_\varepsilon = 1.5$ – safety factors.

Table 1 HP Rotor LCF Lifetime Analysis Results

Point	Baseline Design		Improved Design	
(Fig.10)	ε_a, %	*[N]*	ε_a, %	*[N]*
1	0.2558	320	0.0719	>10000
2	0.1967	1200	0.0606	>10000
3	0.1285	2400	0.0491	>10000
4	0.0508	>10000	0.0498	>10000
5	0.0395	>10000	0.0425	>10000
11	0.0650	>10000	0.0644	>10000

High values of effective strain amplitudes ε_a are observed in monitoring points ‘1’, ‘2’, ‘3’ – under front-end seals carrier. For the baseline design, the maximum amplitude of the deformation has been observed at point ‘1’ and is equal ~ 0.26%, which corresponds to the minimum allowable number of starts from the cold state of 320 and is limited by the potential danger of the LCF crack initiation. Due to changes in the rotor heating conditions, the effective strain range for the most critical zone of the rotor (point ‘1’) was reduced from 0.26 to 0.07%. Consequently, the allowable number of start-ups from the cold state for the HP rotor for the proposed design exceeds 10,000. Similar results were observed throughout the whole area under front-end seals carrier ‘A’ from Fig. 1 – see points ‘2’, ‘3’ in Table 1. For other HP rotor critical regions, the difference in strain range for baseline and modified designs, is not significant and the process of damage accumulation at these points is much slower.

CONCLUSIONS

The research presented in this paper was performed to study the factors and mechanisms influencing the thermal and thermo-structural state for the high-power steam turbine rotor during start-up. As a result, improvements in the thermal and thermo-structural analysis methodology, which enables increased accuracy of the simulations, have been made and are as follows:

- utilization of the improved approach (1D solver) which allows to simulate turbine flow path integrated with gland seal system based on main stream and leakages balance solution, which allows capturing ‘dry’ and ‘saturated’ steam properties, and temperature rise because of ‘Windage’;
- a new correlation for HTC simulation in rotor gland seal groves, based on the experimental evaluations;
- detailed simulation of the rotor front-end seal zone, which allows accounting for the physics of the jet flow;
- film condensation on the steam turbine components surfaces are accounted for.

Applying the developed approach, transient thermal and thermo-structural analyses of the steam turbine K-325-23.5 HP rotor were performed at pre-warming, CS, WS, and HS. The thermal state simulation results showed that during CS, the rotor portion under the front-end seals carrier remains unheated up to the time when the rotor starts to spin. It was also shown that during the CS the rotor is overstressed in the region of the front-end seals.

The significant influence of the steam film condensation and detailed simulation of the physics of the flow in the gland seals on the rotor thermo-stressed state has been confirmed by the comparison against models which do not account for the effects: the difference is 18 and 12% correspondingly.

Based on the performed study, design changes for the front-end seals carrier and heating condition improvements at the pre-warming phase of start-up of the 325 MW steam turbine were made to provide uniform rotor heating and decrease thermo-stresses during turbine start-up from the cold state. Thermo-structural state comparison, which was performed for the modified designs, show that the maximal level of stresses during CS decreased almost 2 times vs. baseline design. LCF analysis for the HP rotor showed that strain range was decreased from 0.256 % (baseline design) to 0.072 % (modified design), which allowed significant increase in the allowable number of steam turbine start-ups from a cold state.

The technology for the improved design was patented [12] and may be used for similar high-powered steam turbines.

ACKNOWLEDGMENTS

We wish to express gratitude to the many people from the A. N. Podgorny Institute for Mechanical Engineering Problems NAS of Ukraine and SoftInWay, Inc. teams, who contributed their time and efforts to perform different experimental, engineering and development tasks related to this work.

REFERENCES

[1] Checcacci, D., Cosi, L., Kumar, S.S. “Rotor life prediction and improvement for steam turbines under cyclic operation”, ASME Turbo Expo 2011, Vancouver, British Columbia, Canada. GT2011-45792.

[2] Moroz, L., Doerksen, G., Romero, F., Kochurov, R., Frolov, B. “Integrated Approach for Steam Turbine Thermo-Structural Analysis and Lifetime Prediction at Transient Operations”, ASME Turbo Expo 2017. Charlotte, NC, USA. GT2017-63547.

[3] Moroz, L., Frolov, B., Kochurov, R. “Steam turbine rotor transient thermo-structural analysis and lifetime prediction”, ASME Turbo Expo 2016. Seoul, South Korea. GT2016-57652.

[4] Brilliant, H.M, Tolpadi, A.K. “Analytical Approach to Steam Turbine Heat Transfer in a Combined Cycle Power Plant”. ASME Turbo Expo. Charlotte, NC, USA. Proceedings of ASME Turbo Expo 2004, Vienna, 2004

[5] Wang, P., Chen, G., Li W. "Improvement in the rapid startup performance for the solar steam turbine", ASME Turbo Expo 2018. Oslo, Norway. GT2018-75174.
[6] Guo, Y., Xie, D. "Thermal stress and deformation analysis of hp casing during shutdown of cpr1000 nuclear steam turbine", ASME Turbo Expo 2017. Charlotte, NC, USA. GT2017-63902.
[7] Jin he "Valve body thermal stress control while warming up", ASME Turbo Expo 2017. Charlotte, NC, USA. GT2017-64126.
[8] Sudakov, A. V., Gavrilov, S. N., Georgievskaja E. V., Levchenko A. I., 2015. "Service Life Extension Substantiation for Steam Turbines with Components which have Deviation from Normative Documentation", Neftegaz.RU. № 1 – in rus.
[9] Incropera, F.P., Dewitt, D.P., 1996, *Fundamentals of Heat and Mass Transfer*, 5th Ed., John Wiley & Sons, Inc., New York, N.Y.
[10] RTM 108.021.103-85. Stationary Steam Turbine Components. Low Cycle Fatigue Analysis. – M.: 1985, № AZ-002/7382, 49p., – in rus.
[11] Matsevity, Yu. M., Alyokhina, S. V., Goloschapov, V. N., Kotulskaja, O. V., 2012, *Heat exchange in construction of steam turbines elements*, NAS of Ukraine, A. N. Podgorny Institute for Mechanical Engineering Problems, Kharkiv, Ukraine. – in rus.
[12] Alekhina S.V., Bakhmutska Yu.O., Goloshchapov V.N., Shvetsov V.L., 2018, "Front-end seals for the high pressure cylinders of high-power steam turbines". Ukrainian Patent № UA 117413 C2. National Academy of Sciences of Ukraine A.Pidgorny Institute of Machanical Engineering Problems, Ukraine: Ministry of economic development and trade of Ukraine.

